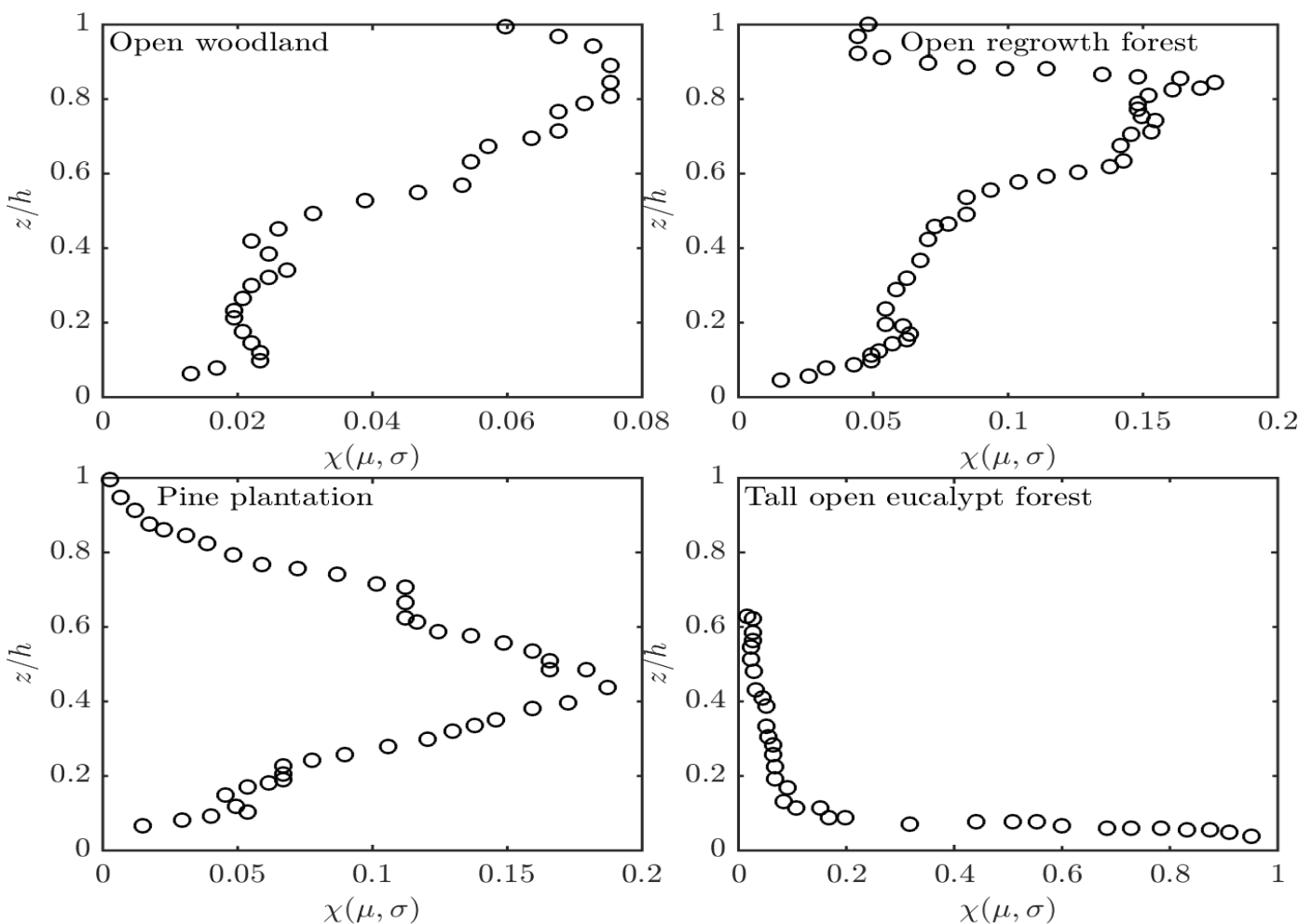




SIMULATIONS OF THE EFFECT OF CANOPY DENSITY PROFILE ON SUB- CANOPY WIND SPEED PROFILES

Duncan Sutherland, Rahul Wadhvani, Jimmy Philip, Andrew Ooi and
Khalid Moinuddin

University of New South Wales, Canberra
Victoria University
The University of Melbourne
Bushfire and Natural Hazards CRC





Version	Release history	Date
1.0	Initial release of document	5/12/2018



Australian Government
**Department of Industry,
 Innovation and Science**

Business
 Cooperative Research
 Centres Programme

All material in this document, except as identified below, is licensed under the Creative Commons Attribution-Non-Commercial 4.0 International Licence.

Material not licensed under the Creative Commons licence:

- Department of Industry, Innovation and Science logo
- Cooperative Research Centres Programme logo
- Bushfire and Natural Hazards CRC logo
- All other logos
- All photographs, graphics and figures

All content not licenced under the Creative Commons licence is all rights reserved. Permission must be sought from the copyright owner to use this material.



Disclaimer:

UNSW Canberra, Victoria University, the University of Melbourne and the Bushfire and Natural Hazards CRC advise that the information contained in this publication comprises general statements based on scientific research. The reader is advised and needs to be aware that such information may be incomplete or unable to be used in any specific situation. No reliance or actions must therefore be made on that information without seeking prior expert professional, scientific and technical advice. To the extent permitted by law, UNSW Canberra, Victoria University, the University of Melbourne and the Bushfire and Natural Hazards CRC (including its employees and consultants) exclude all liability to any person for any consequences, including but not limited to all losses, damages, costs, expenses and any other compensation, arising directly or indirectly from using this publication (in part or in whole) and any information or material contained in it.

Publisher:

Bushfire and Natural Hazards CRC

December 2018

Citation: Sutherland, D., Wadhvani, R., Philip, J., Ooi, A. & Moinuddin, K.A.M. (2018) Simulations of the effect of canopy density profile on sub-canopy wind speed profiles. Melbourne: Bushfire and Natural Hazards CRC.



TABLE OF CONTENTS

ABSTRACT	3
INTRODUCTION	4
NUMERICAL MODEL	6
Large eddy simulation of canopy flows	6
Modelling realistic tree canopies	7
RESULTS AND DISCUSSION	9
Variation in the mean velocity principle	9
Variation in above-canopy flow parameters	11
Quadrant analysis	13
POTENTIAL MODELLING APPROACH	15
CONCLUSIONS	17
ACKNOWLEDGEMENTS	18
REFERENCES	19



ABSTRACT

Duncan Sutherland, *School of PEMS, University of New South Wales, Canberra*

Rahul Wadhvani, *Institute for Sustainable Industries and Liveable Cities, Victoria University*

Jimmy Philip, *Department of Mechanical Engineering, University of Melbourne*

Andrew Ooi, *Department of Mechanical Engineering, University of Melbourne*

Khalid A. M. Moinuddin, *Institute for Sustainable Industries and Liveable Cities, Victoria University*

In computational simulations for weather prediction and fire simulation, forest canopies are often modelled as regions of aerodynamic drag. The magnitude of the drag term depends on the Leaf-Area Density (LAD) of the forest. For most forests LAD varies strongly with height; trees typically have more vegetation at the top of the canopy than the bottom. S. Dupont, and Y. Brunet [Influence of foliar density profile on canopy flow: a large-eddy simulation study. *Agricultural and forest meteorology*, 148(6), pp.976-990. 2008] simulated the flow through three very different profiles of LAD measured from three different Canadian forests. K. Moon, T.J. Duff, and K.G. Tolhurst [Sub-canopy forest winds: understanding wind profiles for fire behaviour simulation, *Fire Safety Journal*, 2016] recently measured the sub-canopy winds and LAD for seven different Australian forest types. Large-Eddy Simulations (LES) of flow through idealised forests are now computationally tractable and an extensive systematic study of different LAD profiles is possible. Here we assume that the LAD can be modelled by a Gaussian with two parameters representing the mean and variance of the distribution of LAD. The total vegetation density is forced to remain constant as the profile changes. We present preliminary simulation results showing how the mean and variance of LAD affects the sub-canopy wind velocity and we discuss a potential modelling approach for sub-canopy wind velocity.



INTRODUCTION

Understanding sub-canopy wind profiles is of crucial importance to parameterising the atmospheric boundary layer above a forest canopy and also estimating wind reduction factors for fire spread models. An analytic model exists for large, uniform canopy. That is, the occupied volume fraction, or leaf area density (LAD) of the canopy is constant over the whole canopy. The model of Inoue [1963] is based on a balance between turbulent stresses and the drag force of the canopy. Harman and Finnigan [2007] significantly extended the Inoue model to include the above canopy flow and non-neutral atmospheric conditions. Similar to Inoue, their model assumes a very large forest, free of any forest edges or inhomogeneity in the forest canopy. The model has two empirical parameters that are straightforward to measure. The model requires only the canopy top velocity and the leaf area index of the forest to predict the sub-canopy profile in neutral atmospheric conditions.

In nature, there is strong variation of LAD in all three spatial directions; the variation is most prominent in the vertical direction because trees typically have more vegetation at the top of the canopy than the bottom. A limited investigation of the effect of vertical distribution of LAD on the sub-canopy wind profiles was conducted [Dupont et al. 2008]. Three different observed profiles of LAD from different forests were used and the profiles were scaled to give a range of five different leaf area indices (LAI or integrated LAD). Dupont et al. drew several important conclusions from this study: the gross features of the above canopy flow are unchanged by canopy profile; increasing the LAI makes the features of the canopy flow more pronounced; finally there is considerable variation in the mean flow and turbulent profiles in the sub-canopy space. That is, close to the ground the difference in flow and turbulence profiles caused by different LAD profiles are seen more clearly.

Recently, Moon et al. [2016] performed field measurements of sub-canopy wind speeds in Australian vegetation. The measurements of LAD by Moon et al. [2016], and similar measurements made by Amiro [1990], show considerable variability in the LAD profiles for different forest types around the world. Some of the measured profiles obtained by Moon are shown in figure 1. Dupont et al. [2008] conducted simulations of canopy flow with three distinct LAD profiles similar to the spruce, pine, and aspen forests measured by Amiro [1990]. Here we parameterise forests with a Gaussian LAD, systematically vary the mean and variance of the LAD distribution, and analyse the resulting sub-canopy flow with an eye towards constructing simplified models of the sub-canopy wind profile. Systematically varying the parameterisation of a forest canopy to determine a simplified model of the sub-canopy profile follows the methodology of Zhu et al. [2016]. Zhu et al. [2016] used LES to simulate the flow over numerous synthetic urban canopies with varying mean, variance, skewness, and kurtosis of the topography distribution.

In this study, we use Fire Dynamics Simulator (FDS) [McGrattan et al., 2013] to conduct large eddy simulations (LES) of the sub- and above canopy flow. FDS has been shown to reproduce experimental and simulation results for flows over homogeneous canopies [Mueller et al., 2014]. LES has recently become a standard tool for investigating atmospheric flows and flows over both forest and

urban canopies in multiple configurations. Most LES studies assume an approximately Gaussian LAD distribution for example: Cassiani et al., [2008], Kanani-Suhring and Raasch, [2017], Dupont and co-workers [2008, 2011]; although, unlike the present study, the mean and variance of the LAD profiles were not changed in those studies. In the next section we briefly discuss the LES methodology and the model of the forest canopy that was used in this study, then we present the sub-canopy wind profiles, and finally we discuss adapting the model of Inoue [1963] and subsequently the model of Harman and Finnigan [2007] to account for vertical variation in LAD.

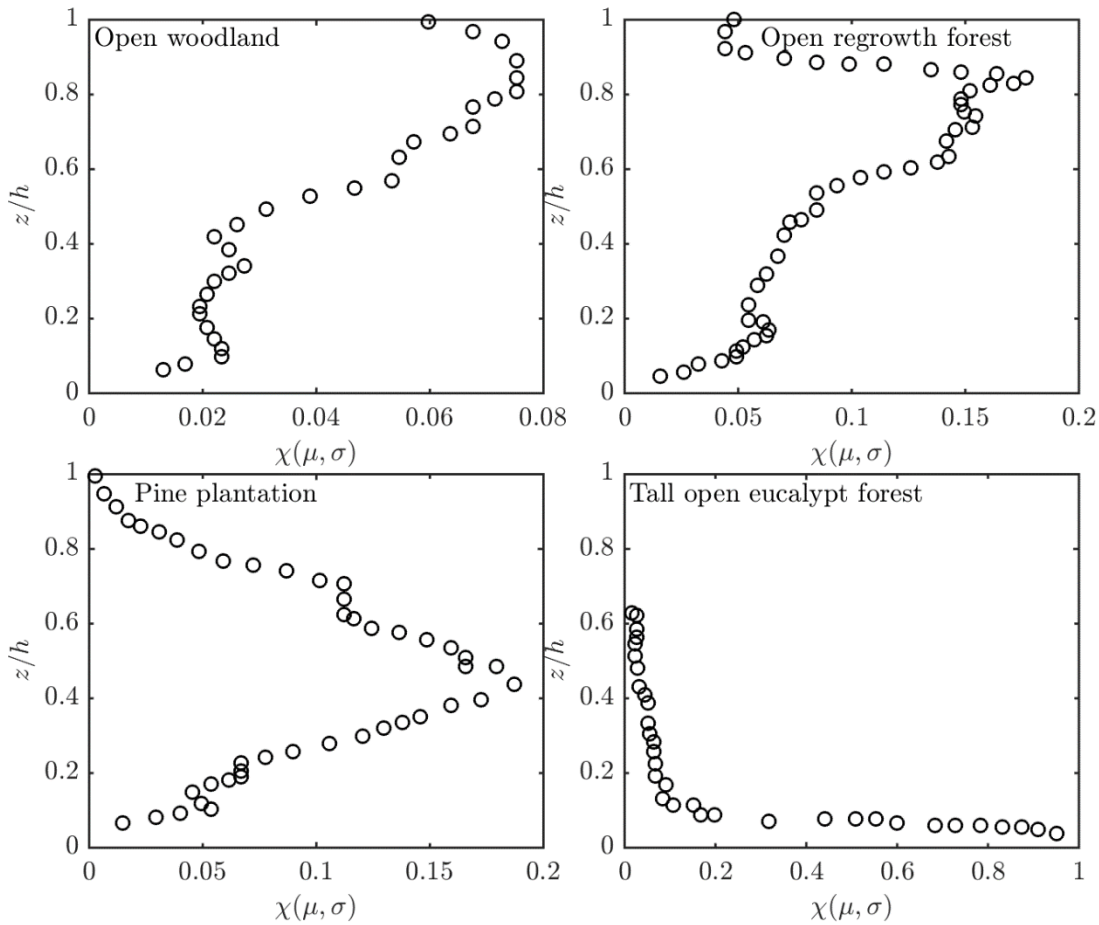


Figure 1: Profiles of LAD measured by Moon et al. [2016] for four different forest types

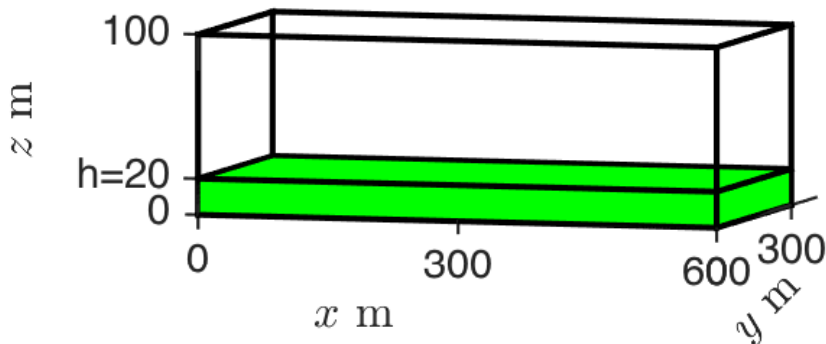


Figure 2: The simulation domain showing the canopy region, shaded in green. the boundaries in the x - and y -directions are periodic, the top boundary is free slip and the bottom is a no-slip boundary.

NUMERICAL MODEL

LARGE EDDY SIMULATION OF CANOPY FLOWS

In LES, the continuity and Navier-Stokes equations are spatially filtered to retain the dynamically important large-scale structures of the flow. In FDS, the filtering operation is implicit at the grid scale. The largest eddies contain the most energy and therefore make the largest contribution to momentum transport. The diffusive effect of the unresolved small scales on the resolved large scales is non negligible. The constant Smagorinsky sub-grid-scale stress model (see, for example, Pope, 2001) is used in this work with the Smagorinsky constant set to $C = 0.1$ [Lesieur et al., 2005]. The flow is maintained by a pressure gradient equal to 0.005 Pa/m . The fluid is assumed to be air with density $\rho = 1.225 \text{ kg/m}^3$ and viscosity $\nu = 1.8 \times 10^{-5} \text{ m}^2\text{s}^{-1}$.

For completeness, the LES equations are:

$$\frac{\partial u_i}{\partial t} + u_j \left(\frac{\partial u_i}{\partial x_j} + \frac{\partial u_j}{\partial x_i} \right) = \frac{1}{\rho} \frac{\partial p}{\partial x_j} + \frac{\partial \tau_{i,j}}{\partial x_j} + F_{D,i} + \frac{1}{\rho_0} (\rho - \rho_0) g_i,$$

$$\frac{\partial \rho}{\partial t} + u_i \frac{\partial \rho}{\partial x_j} = k \frac{\partial^2 \rho}{\partial^2 x_j},$$

where u_i is the resolved part of the velocities, $i, j = x, y, z$ are the coordinates, ρ is the fluid density, p is (the modified) pressure, and τ_{ij} is defined as:

$$\tau_{i,j} = -2(\nu + \nu_t) S_{i,j} + 3 \frac{\partial u_i}{\partial x_i} \delta_{i,j},$$

where $S_{i,j}$ is the rate of strain tensor, $\delta_{i,j}$ is one if i and j are equal, and zero otherwise.

$$\nu_t = -2(C\Delta)^2 |S| S_{i,j},$$

$$S_{i,j} = \frac{1}{2} \left(\frac{\partial u_i}{\partial x_j} + \frac{\partial u_j}{\partial x_i} \right),$$

where $\Delta = (\delta x \delta y \delta z)^{1/3}$ is a measure of grid spacing.

Following Dupont et al. [2011] the canopy of height h is modelled as an aerodynamic drag term of the form

$$F_{D,i,k}(x, z) = \rho c_D \chi(z, h, \mu, \sigma, A, B) (u_j u_j)^{1/2} u_j.$$

The value of the drag coefficient is taken to be $c_D = 0.25$ roughly consistent with the measurements of Amiro [1990] and the study of Cassiani et al. [2008]. The function $\chi(z, h, \mu, \sigma, A, B)$, defines the spatial location of the canopy. The canopy is assumed to have a constant height across the whole domain. Below the canopy height there is some LAD profile. In this study the LAD is assumed to be

a Gaussian with some specified geometric mean μ and some variance σ . Physically, μ corresponds to the height at which the canopy is most dense; σ roughly measures the width of the leafiest part of the tree crowns.

$A + B$ is the maximum value of the LAD. B is a uniform contribution to LAD; it may be supposed that B represents the contribution to LAD from the tree trunks.

The LAD profile is:

$$\chi(z, h, \mu, \sigma, A, B) = \begin{cases} A \exp\left(-\frac{(z - \mu)^2}{\sigma^2}\right) + B, & z \leq h, \\ 0, & z > h \end{cases}$$

The height of the canopy is taken as $h = 20$ m and h is a natural length scale of the flow. The choice of μ, σ, A , and B , will be discussed in the next section.

The size of the exterior domain is chosen so that the largest relevant structures are captured. The channel sizes are chosen to follow the proportions set out by Moser et al. [1999]. Bou-Zeid et al. [2009] recommends the channel height be at least four times larger than the canopy height to prevent artificial flow acceleration between the top boundary and the canopy. The overall domain size is $600 \times 300 \times 100$ m ($30h \times 15h \times 5h$). The streamwise and spanwise boundary conditions are periodic. The bottom (ground) boundary condition is enforced using the log-law of the wall [Bou-Zeid et al., 2004]. The log-law of the wall is used at the bottom boundary [Belcher et al., 2003] and the log-law of the wall is enforced using a Werner-Wenkle approximation [McGrattan et al., 2013]. The normal velocity is forced to vanish at the top of the domain.

The resolution of the simulation 5 m in the horizontal directions and 0.5 stretched to 4 m at the top of the domain. The resolution is approximately three times finer than the resolution used by Bou-Zeid et al. [2009]. A sketch of the simulation domain and the canopy location is shown in figure 2.

The flow is initialised from a uniform velocity with a random perturbation to ensure tripping to a turbulent flow. The flow is allowed to develop to a statistically stationary state over approximately 3600 s and statistics are sampled every 2 s for 7200 s. The total simulation time was selected to ensure relatively smooth derivatives of the mean velocity profiles.

MODELLING REALISTIC TREE CANOPIES

The canopy model used here, $\chi(z, h, \mu, \sigma, A, B)$, is a five parameter model. We firstly assume that h is constant which reduces number of parameters to four. The Leaf Area Index (LAI), that is integral of LAD with respect to z over the canopy, is also fixed and for this report we consider only $LAI = 1$. This gives:

$$A = \frac{1 - Bh}{\int_0^h \exp\left(-\frac{(z - \mu)^2}{\sigma^2}\right) dz}$$

Because A is considered to be positive, $B < \frac{1}{h}$, which physically means a canopy of $LAI=1$ cannot be constructed only from the 'trunks' of trees. We somewhat

arbitrarily assumed that the trunks contribute approximately 10% of the LAD and therefore we fixed $\frac{B}{A} = 0.1$. This assumption was partly justified by fitting profiles to the measurements of Moon et al. Therefore the parameter space is $(LAI, \frac{A}{B}, \mu, \sigma)$ where $(LAI, \frac{A}{B})$ were fixed at some physically reasonable value and (μ, σ) were varied in this study. The effects of varying LAI and $\frac{B}{A}$ on the sub-canopy profile are the subjects of ongoing research.

Profiles of LAD are shown in figure 3. The profiles in figure 3(a) were obtained by setting the variance σ^2 to its minimum value and then varying μ . The profiles in figure 3(b) were obtained by setting μ to its maximum value and varying σ^2 . The black line is the same in both plots. The simulation cases are tabulated in table 1. Notice that the red profile in figure 3(a) somewhat resembles the old growth eucalyptus profile measured by Moon et al. [2016] and the red profile in figure 3(b) somewhat resembles the open regrowth forest profile measured by Moon et al. [2016], although the observed profiles have different maxima.

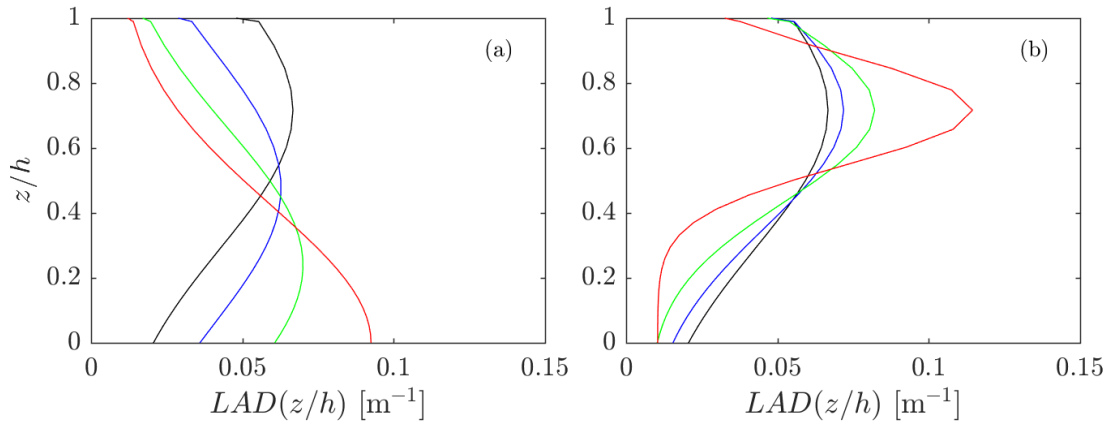


Figure 3: Sample of LAD profiles used in this study. In (a) $\sigma^2=0.325$ is held constant and $\mu=0.00$ (red), 0.233 (green), 0.467 (blue), and 0.700 (black). in (b) $\mu=0.70$ is constant and $\sigma^2=0.325$ (black – the same curve as in (a)), 0.233 (blue), 0.142 (green), and 0.050 (red)

Table 1: Simulation LAD parameters for all cases

LAI	μ	σ^2	A	B/A
1.000	0.700	0.050	0.104	0.100
1.000	0.700	0.142	0.075	0.100
1.000	0.700	0.233	0.065	0.100
1.000	0.700	0.325	0.061	0.100
1.000	0.000	0.325	0.084	0.100
1.000	0.233	0.325	0.064	0.100
1.000	0.467	0.325	0.057	0.100

RESULTS AND DISCUSSION

VARIATION IN THE MEAN VELOCITY PRINCIPLE

As is standard in the analysis of turbulent flows the instantaneous velocity fields are decomposed into average and fluctuating quantities. That is,

$$u = \bar{u} + \tilde{u},$$

and so on for the other velocity components. The overbar denotes averaging in the x – and y –directions and in time. The fluctuations \tilde{u} are subsequently averaged in time and the time-averaged fluctuations are denoted u' . For convenience we will adopt the convention that $u_1 = u, u_2 = v, u_3 = w$. The friction velocity at the canopy top is defined as

$$u_* = \sqrt{\frac{\tau_{1,3}(h)}{\rho}}.$$

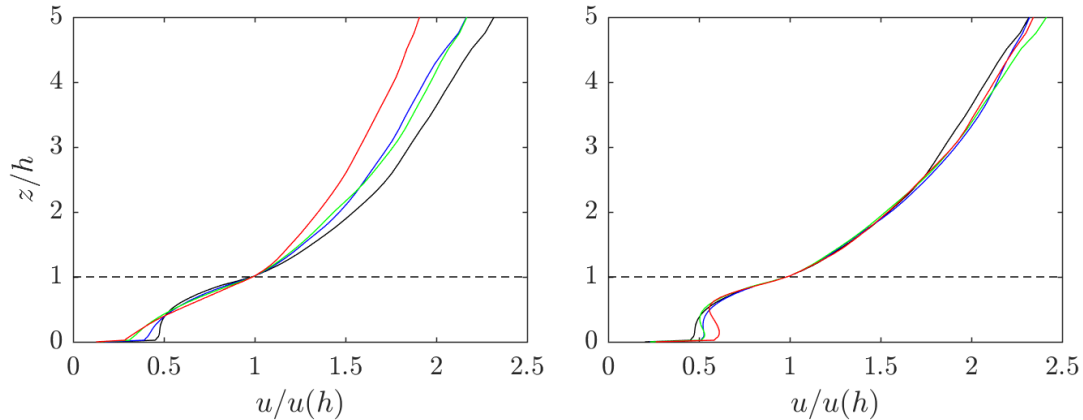


Figure 4: Normalised drag force throughout the canopy. The canopy lad profiles are the same as shown in Figure 3. That is, in (a) $\sigma^2=0.325$ is held constant and $\mu=0.00$ (red), 0.233 (green), 0.467 (blue), and 0.700 (black). in (b) $\mu=0.70$ is constant and $\sigma^2=0.32325$ (black – the same curve as in (a)), 0.233 (blue), 0.142 (green), and 0.050 (red). The dotted line is the profile that exerts the greatest total drag, that is, the profile that encloses the greatest area to the left of the curve.

The simulated mean wind profiles are shown in figure 4. The profiles are all normalized by the value of the wind speed at the top of the canopy at $z/h = 1$, that is, at $z/h = 1$, $u/u(h)$ is also 1. The pressure gradient and LAI are held constant during these simulations. The variation of the LAD profile leads to variation in the drag force exerted by the canopy upon the fluid. It is difficult to appreciate the drag forces by studying only the normalised velocity profiles in figure 4. Because the LAD profile is known and the average sub-canopy wind velocity is simulated, the LAD profile, that gives the maximum drag force, can be measured. The profiles of drag force are plotted in figure 5. In these simulations, the canopy which exerts the maximum drag force is $\mu = 0.7, \sigma^2 = 0.05$. That is the profile with maximum mean and minimum variance. This result indicates that the canopies that exert the most drag force concentrate leaf material high in the canopy where the incident velocity is greatest. Evident in figure 4(b) is a

significant local maximum at approximately $z/h = 0.3$ for the profile with $\mu = 0.7$, $\sigma^2 = 0.05$, even though this particular canopy exerts the most drag on the flow. Examining the average drag force (figure 5) shows that for the $\mu = 0.7$, $\sigma^2 = 0.05$ canopy the drag force is minimal and constant for $z/h < 0.4$ and due to the absence of drag forces on the fluid the pressure gradient driven flow achieves a maximum in the trunk space.

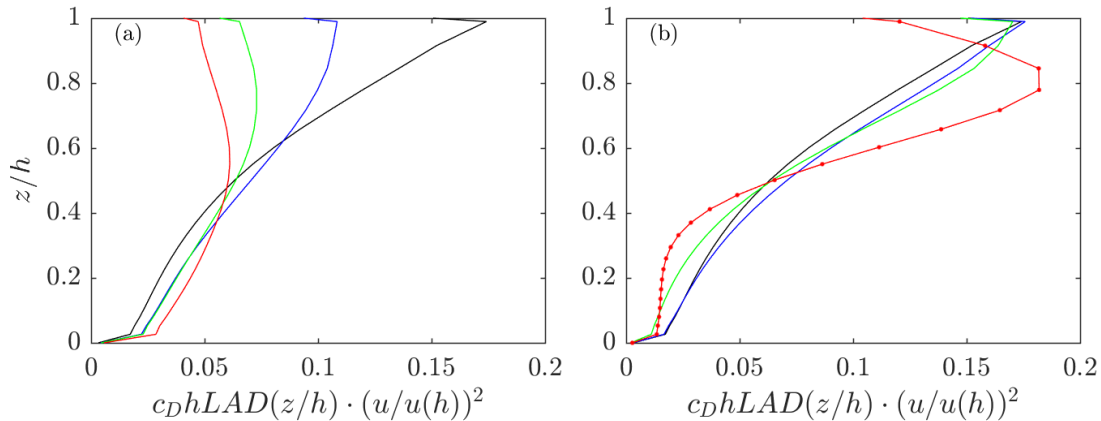


Figure 5: Normalised drag force throughout the canopy. The canopy LAD profiles are the same as shown in Figure 3. That is, in (a) $\sigma^2=0.325$ is held constant and $\mu= 0.00$ (red), 0.233 (green), 0.467 (blue), and 0.700 (black). In (b) $\mu=0.70$ is constant and $\sigma^2=0.32$ (black – the same curve as in (a)), 0.233 (blue), 0.142 (green), and 0.050 (red). The dotted line is the profile that exerts the greatest total drag, that is, the profile that encloses the greatest area to the left of the curve.

The local maximum of velocity is likely to be a consequence of using an imposed pressure gradient to drive the mean flow through the domain.

Reynolds shear stress $-u'w'$ is the product of the fluctuations in the streamwise and vertical directions and is used to quantify the effect of turbulence in the flow. The Reynolds shear stresses normalized by the canopy top friction velocity are plotted in figure 6. The Reynolds shear stress exhibits linear behavior above the canopy as is expected for pressure gradient driven flows [Bou-Zeid et al. 2004] and decays rapidly within the canopy, consistent with the simulations of Mueller et al. [2014].

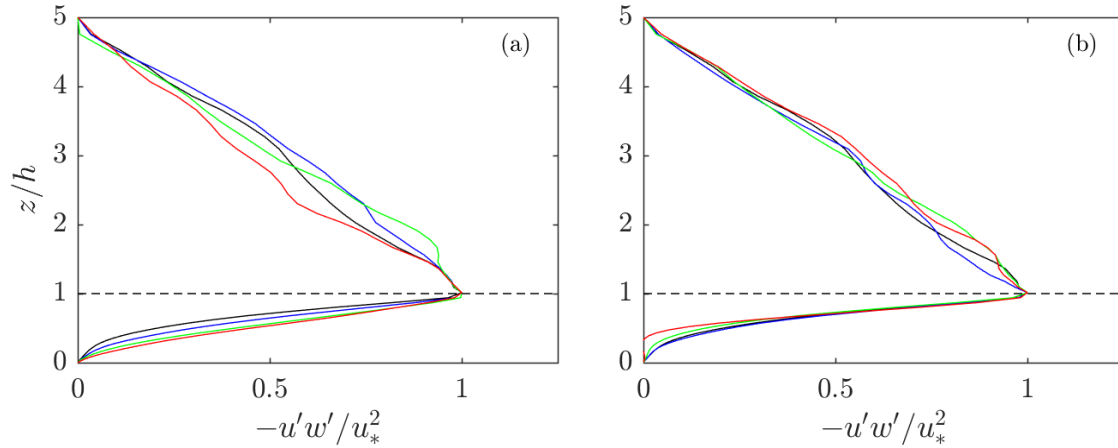


Figure 6: Reynolds shear stress profiles normalised by the friction velocity at the canopy. The canopy LAD profiles are the same as shown in Figure 3. That is, in (a) $\sigma^2=0.325$ is held constant and $\mu=0.00$ (red), 0.233 (green), 0.467 (blue), and 0.700 (black). In (b) $\mu=0.70$ is constant and $\sigma^2=0.325$ (black – the same curve as in (a)), 0.233 (blue), 0.142 (green), and 0.050 (red).

VARIATION IN ABOVE-CANOPY FLOW PARAMETERS

The Harman and Finnigan [2007] model for neutral flow over a canopy with known LAI and drag coefficient relies on three parameters: β the ratio of shear stress to u –velocity at the canopy top, z_0 the equivalent roughness length of the canopy, and d the displacement height of the canopy. The three parameters may be measured from our simulations. The computed β are shown in figure 7, d in figure 8, and z_0 in figure 9 all plotted against the canopy parameters μ and σ^2 . β shows weak linear growth with μ and is approximately constant with σ^2 . The observations of Harman and Finnigan [2007] suggest that β is constant independent of the canopy LAD distribution. The β values (approximately $\beta = 0.2$) simulated here are lower than typically observed for these flows, nonetheless, the values observed here are consistent with those observed $\beta = 0.3$ by Harman and Finnigan [2007] and Mueller et al. [2014] observe simulated values close to $\beta = 0.3$. The reason for the lower values observed here may be due to Reynolds number effects. The canopy top velocities (of the order 2 ms^{-1}) simulated here are approximately twice the canopy top velocities simulated by Mueller et al. Further work is required to explore the possible Reynolds number dependence of $\beta = 0.3$. The displacement length d by is estimated using the centroid of drag force [Garratt,1992]

$$d = \frac{\int_0^h z (A \exp\left(-\frac{(z-\mu)^2}{\sigma^2}\right) + B) \bar{u}^2 dz}{\int_0^h (A \exp\left(-\frac{(z-\mu)^2}{\sigma^2}\right) + B) \bar{u}^2 dz}.$$

The values of simulated displacement length are of the same order as experimentally observed [Dolman, 1986]. As could be expected, the displacement length exhibits strong linear variation with canopy parameters μ and σ^2 . The displacement length increases with increasing μ as LAD becomes concentrated at greater heights, similarly the displacement length decreases

with increasing σ^2 as the LAD is distributed over a larger range of heights. The roughness length z_0 was determined from a least-squares regression fit to the average velocity data above the canopy. The functional form of velocity profile that was fitted was a standard log-law [Zhu et al. 2016]

$$u = \frac{u_*}{\kappa} \log \frac{z-d}{z_0},$$

where $\kappa = 0.38$ is von Karman's constant. The fitted values for z_0 are in agreement with the observations of Dolman [1986] and the values obtained for z_0 do not exhibit strong variation with the canopy parameters. These results suggest that μ , the geometric mean of LAD, is the only parameter that significantly influences the above-canopy flow through the displacement length.

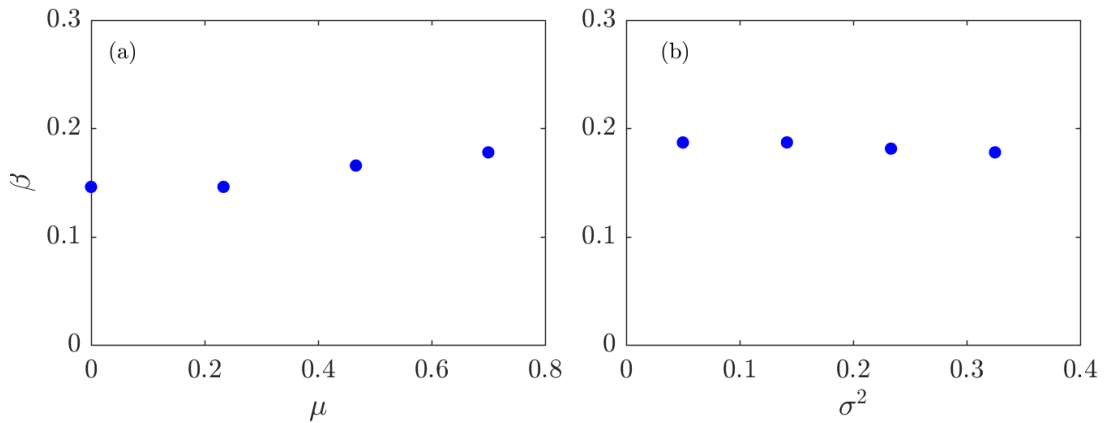


Figure 7: β parameter variation with (a) μ , and (b) σ^2

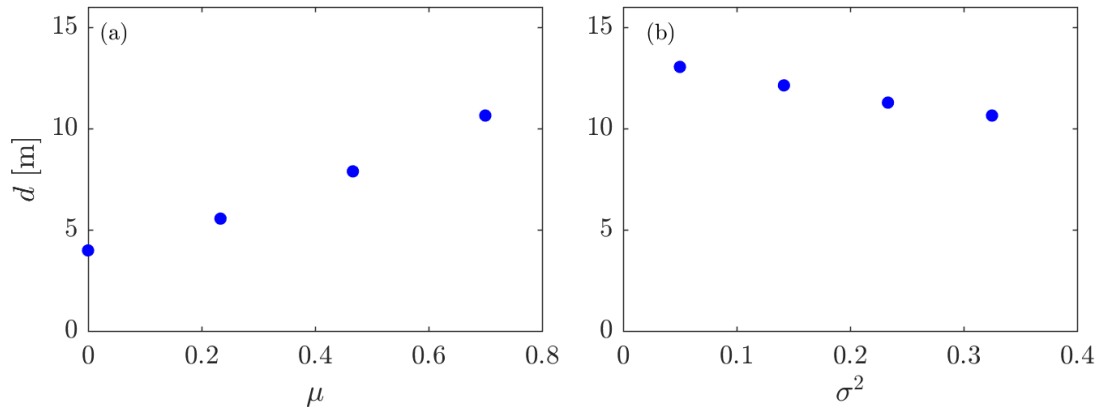


Figure 8: d displacement length variation with (a) μ , and (b) σ^2

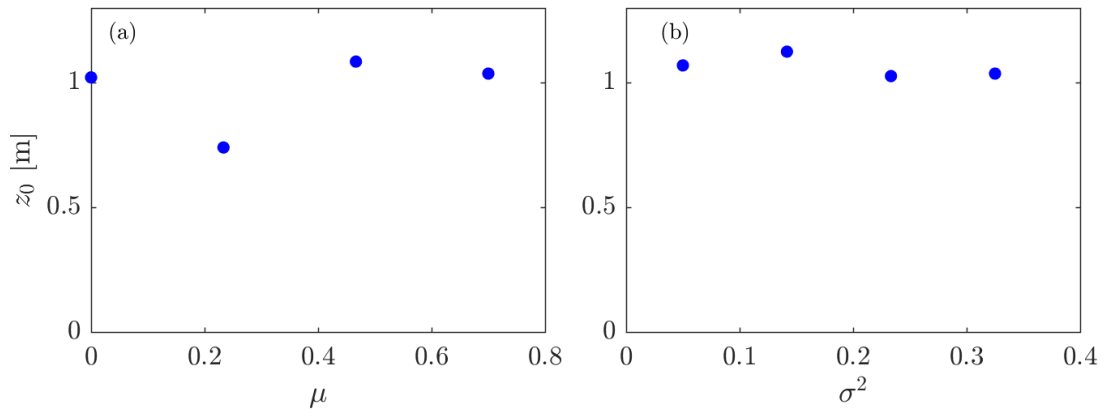


Figure 9: z_0 roughness length variation with (a) μ , and (b) σ^2

QUADRANT ANALYSIS

The characteristics of the turbulent flow within and immediately above the canopy have implications for simulating ember transport in wildfires. Embers are often modelled as Lagrangian particles and modern Lagrangian particle transport models use quadrant analysis of the sweep-ejection cycle to parameterise the forces to turbulent fluctuations that act upon the particle. The probability distribution of turbulent fluctuations $P(u', w')$ in the x – and z – directions are classified, by the quadrants of the distribution, into outward interactions, ejections, inward interactions, and sweeps. The ejections and sweeps are the most important of these motions. Ejections are the motion of coherent structures upwards and in the x –direction of the mean flow out of the canopy, whereas sweeps are motions downwards into the canopy in the x –direction. Jinn et al. [2015] have developed a model of particle transport over a smooth surface which parameterises the turbulent forces on the particle using $P(u', w')$. Canopy flow is dominated by sweeping motions at the canopy top [Finnigan, 2000]. Hence it is worthwhile to examine the effect of LAD parameters on the sweep-ejection cycle and on the distribution of turbulent fluctuations $P(u', w')$. The contours of $P(u', w')$ at $z = h$ are shown in figure 11. As expected sweeping motions dominate the distribution and increasing μ enhances sweeping motions, however, variations in σ^2 appear to have only marginal effects on $P(u', w')$.

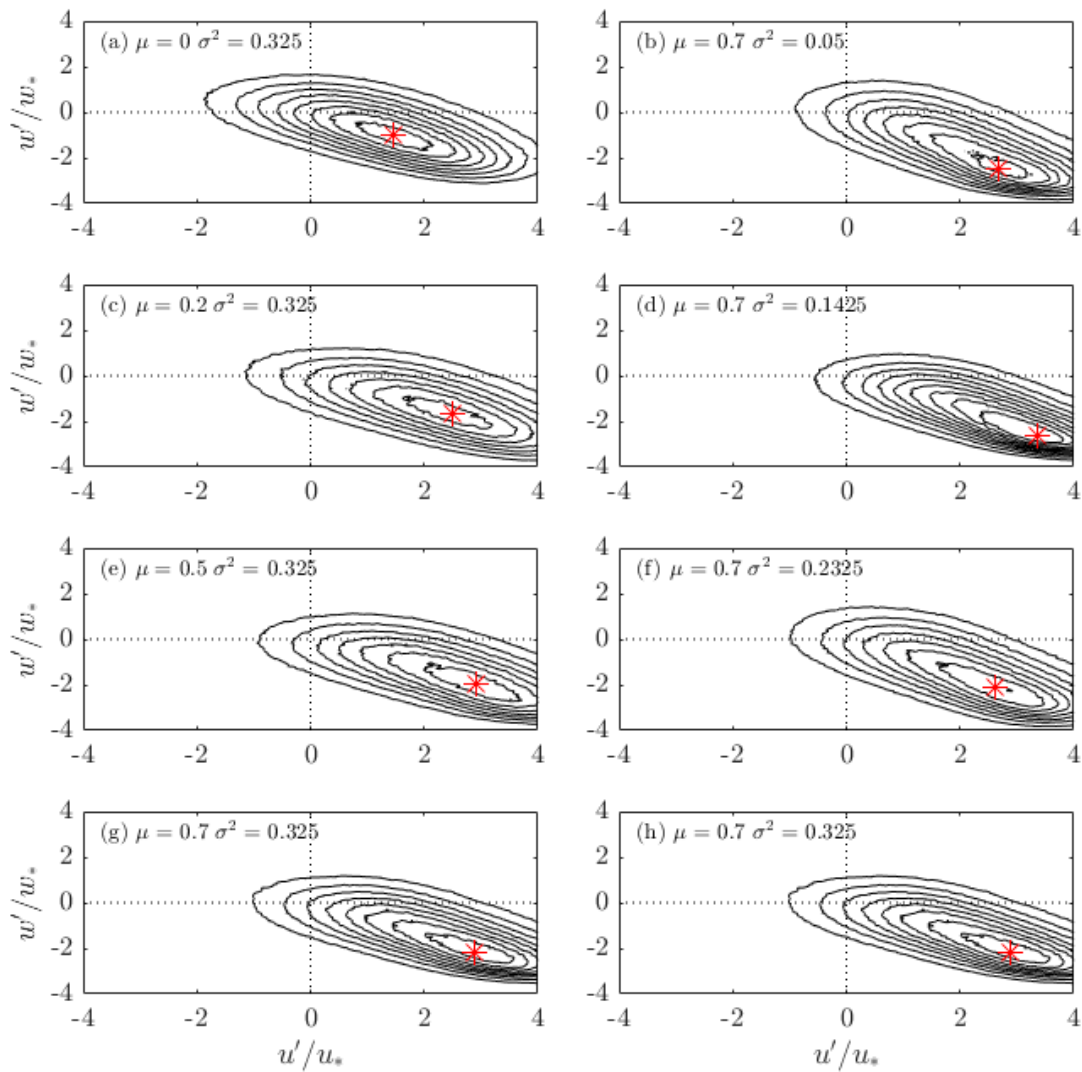


Figure 10: Quadrants of $P(u', w')$ for the respective canopy cases. Sweeps are where $u' > 0$ and $w' < 0$. Note that the red star is the location of the peak in $P(u', w')$ and, to guide help the eye, the plot in (g) is repeated in (h).

POTENTIAL MODELLING APPROACH

Inoue [1963] developed a momentum-balance model to determine the sub-canopy wind profiles deep within a canopy. Harman and Finnigan [2007] extend the original model of Inoue to blend smoothly with a roughness sub-layer and logarithmic layer above the canopy and incorporates the effects of atmospheric stability. The discussion here will follow Harman and Finnigan [2007].

The Navier-Stokes equations may be averaged in time and in space for a LAD that is constant in the x -, y -, and z -directions. For convenience the canopy top is located at $z = 0$. At the end of the derivation we will apply a coordinate transform to recover the canopy top at $z = h$. The canopy is thought of as infinitely deep. The averaging process removes the time derivative and the advection terms from the Navier-Stokes equations. The pressure gradient term is also assumed to be negligible relative to the turbulent stress term and the drag term. The momentum balance is then

$$\frac{\partial \tau_{x,z}}{\partial z} + F_{D,x} = 0,$$

where we have written the coordinates explicitly instead of i, j, k . The turbulent stress term may then be modelled using the mixing length approximation. The drag term is modeled as before, however, we assume that the canopy has uniform leaf area index. This gives the following ordinary differential equation

$$\frac{\partial}{\partial z} l^2 \frac{\partial}{\partial z} u + c_d LAI u^2 = 0,$$

Boundary conditions are that the velocity derivative vanishes as $z \rightarrow \infty$ and the canopy top velocity U_h is known. The equation has solution:

$$u = U_h \exp \frac{\beta z}{l},$$

Scaling arguments which depend on a constant LAD profile show that the mixing length is $l = 2\beta^3 / c_d LAI$. Harman and Finnigan [2007] showed that the exponential profile agrees sufficiently well with observed subcanopy profiles. The most commonly violated assumption of the Inoue model is the canopy has finite depth. In practical terms, the Inoue model works for the top part of the canopy and progressively makes poor predictions near the ground. In these simulations there is the presence of a driving pressure gradient and LAD is not constant in the z -direction. Hence we expect that the model of Inoue [1963] will give poor agreement through the canopy.

The resulting sub-canopy model is tested by comparing the simulated sub-canopy velocity profiles with the modelled profiles using the firstly the simulated values of β (figure 8) and the value $\beta=0.3$ observed by Harman and Finnigan [2007]. The comparison between the simulated and modelled profiles are shown in figure 12(a) and (b). The modelled profiles with the simulated value of β do not agree well with the simulated profiles. However, using the value of $\beta=0.3$ observed by Harman and Finnigan [2007] improves the agreement in the top half

of the canopy. Nonetheless, β must be considered a parameter of the model rather than some universal constant.

To reduce the discrepancy between the modelled and simulated profiles we attempt to address the assumption of a constant LAD profile. Because the displacement length is the only quantity that varies significantly with the canopy parameters, it is hypothesised that d is a more relevant length scale than the constant canopy height h . Therefore we define the displacement length Leaf Area Index $dLAI$ as

$$dLAI = \int_0^d A \exp\left(-\frac{(z-\mu)^2}{\sigma^2}\right) + B dz,$$

that is, the leaf area index computed from $z = 0$ to $z = d$ instead of $z = h$. The $dLAI$ is then used in place of LAI in the Inoue model. The modified model predictions, using the simulated values of β , are compared to the simulated profiles in figure 12(c) and (d). Agreement between the modeled and simulated profiles in the top half of the canopy is significant but far from perfect. The modelled profiles do not agree with the simulated in the bottom half of the canopy and further work is required to improve the Inoue model in the near ground region.

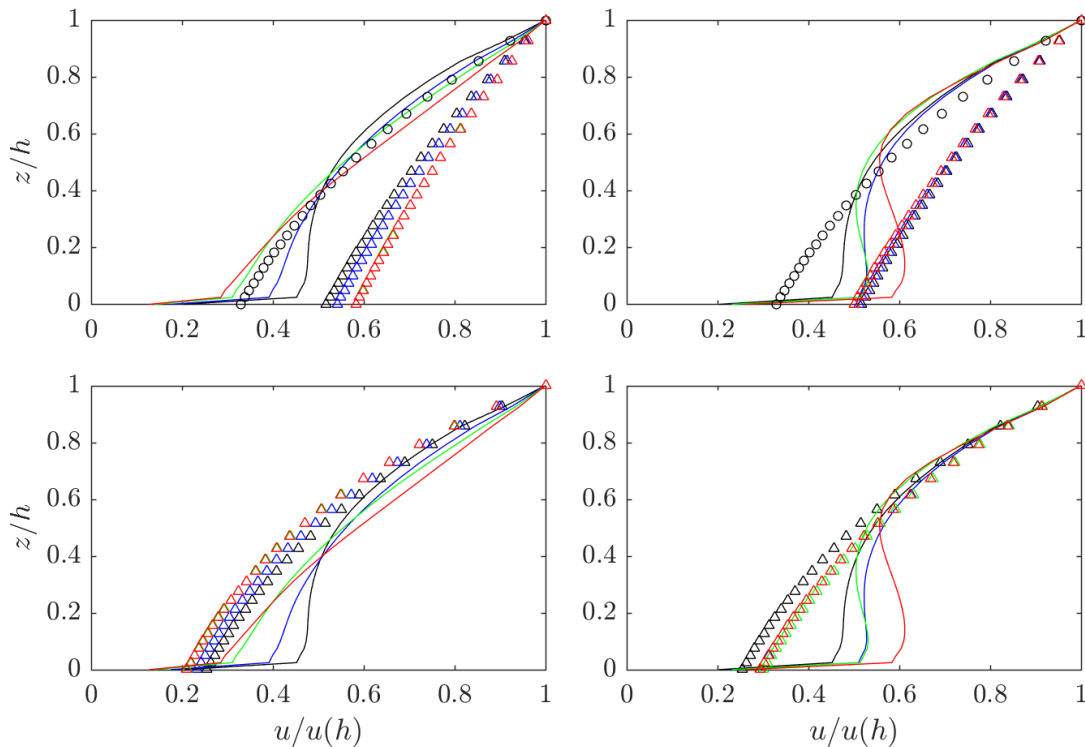


Figure 11: Modelled and simulated sub-canopy u –velocity profiles. (a and b) contain the modelled profiles using the simulated β (triangle symbols) and the observed β (circle symbol) of Harman and Finnigan [2007] and a constant mixing length based on LAI . The modelled profiles in (c and d) use the simulated β and $dLAI$. The canopy LAD profiles are the same as shown in figure 3. That is, in (a) $\sigma^2=0.325$ is held constant and $\mu=0.00$ (red), 0.233 (green), 0.467 (blue), and 0.700 (black). In (b) $\mu=0.70$ is constant and $\sigma^2=0.325$ (black – the same curve as in (a)), 0.233 (blue), 0.142 (green), and 0.050 (red). (c) and (d) are the same curves as (a) and (b) respectively.



CONCLUSIONS

The effect of LAD distribution on flow over a tree canopy was investigated using LES. The geometric mean μ and variance σ^2 of the LAD distribution were varied independently. The sub-canopy mean flow profile was found to be sensitive to both μ and σ^2 , with the emergence of a prominent sub-canopy peak of u -velocity. The parameters of the above canopy flow, namely β the ratio of shear stress to u -velocity at the canopy top and z_0 the equivalent roughness length of the canopy, and d the displacement length, were found to be largely independent of σ^2 . β exhibits a weak dependence on μ but z_0 appears to be independent of both μ and σ^2 . The displacement length exhibits strong linear dependence μ and a weaker linear dependence on σ^2 . The turbulent fluctuations at the canopy top are characterized using quadrant analysis, with an eye towards modeling particle transport across the canopy. Sweeping motions dominate the flow with increasing μ enhancing the sweeping motions. Finally the sub-canopy u -velocity model of Inoue [1963] was improved by including the displacement length.



ACKNOWLEDGEMENTS

The authors are grateful to the administrators of Spartan, a high-performance computing cluster at the University of Melbourne.



REFERENCES

- B.D. Amiro. Comparison of turbulence statistics within three boreal forest canopies. *Boundary-Layer Meteorology*, 51(1-2):99–121, 1990.
- SE Belcher, N Jerram, and JCR Hunt. Adjustment of a turbulent boundary layer to a canopy of roughness elements. *Journal of Fluid Mechanics*, 488:369–398, 2003.
- E. Bou-Zeid, C. Meneveau, and M.B. Parlange. Large-eddy simulation of neutral atmospheric boundary layer flow over heterogeneous surfaces: Blending height and effective surface roughness. *Water Resources Research*, 40(2), 2004.
- E. Bou-Zeid, J. Overney, B. D. Rogers, and M. B. Parlange. The effects of building representation and clustering in large-eddy simulations of flows in urban canopies. *Boundary-layer meteorology*, 132(3):415–436, 2009.
- M. Cassiani, G.G. Katul, and J.D. Albertson. The effects of canopy leaf area index on airflow across forest edges: large-eddy simulation and analytical results. *Boundary-layer meteorology*, 126(3):433–460, 2008.
- A.J. Dolman, Estimates of roughness length and zero plane displacement for a foliated and non-foliated oak canopy. *Agricultural and forest Meteorology*, 36(3), pp.241-248, 1986.
- S. Dupont, and Y. Brunet, Influence of foliar density profile on canopy flow: a large-eddy simulation study. *Agricultural and forest meteorology*, 148(6), pp.976-990, 2008.
- S. Dupont, J-M. Bonnefond, M. R. Irvine, E. Lamaud, and Y. Brunet. Long-distance edge effects in a pine forest with a deep and sparse trunk space: in situ and numerical experiments. *Agricultural and Forest Meteorology*, 151(3):328–344, 2011.
- J. Finnigan, Turbulence in plant canopies. *Annual review of fluid mechanics*, 32(1), pp.519-571, 2000.
- I.N. Harman and J. J. Finnigan. A simple unified theory for flow in the canopy and roughness sublayer. *Boundary-layer meteorology*, 123(2):339–363, 2007.
- E. Inoue. On the turbulent structure of airflow within crop canopies. *Journal of the Meteorological Society of Japan. Ser. II*, 41(6):317–326, 1963.
- C. Jin, I. Potts, and M.W. Reeks. A simple stochastic quadrant model for the transport and deposition of particles in turbulent boundary layers. *Physics of Fluids*, 27(5), p.053305. 2015
- F. Kanani-Suhring and S. Raasch. Enhanced scalar concentrations and fluxes in the lee of forest patches: A large-eddy simulation study. *Boundary-Layer Meteorology*, pages 1–17, 2017.
- K. McGrattan, S. Hostikka, and J.E. Floyd. Fire dynamics simulator, users guide. NIST special publication, 1019, 2013.
- K. Moon, T.J. Duff, and K.G. Tolhurst. Sub-canopy forest winds: understanding wind profiles for fire behaviour simulation. *Fire Safety Journal*, 2016.
- E. Mueller, W. Mell, and A. Simeoni. Large eddy simulation of forest canopy flow for wildland fire modeling. *Canadian Journal of Forest Research*, 44(12):1534–1544, 2014.
- X. Zhu, G.V. Iungo, S. Leonardi, and W. Anderson. Parametric study of urban-like topographic statistical moments relevant to a priori modelling of bulk aerodynamic parameters. *Boundary-Layer Meteorology*, 162(2), pp.231-253, 2017.